

## A 2.4 Gb/s Millimeter-Wave Link Using Adaptive Spatial Multiplexing

Colin Sheldon\*<sup>(1)</sup>, Munkyo Seo<sup>(2)</sup>, Eric Torkildson<sup>(3)</sup>, Upamanyu Madhow<sup>(3)</sup> and Mark Rodwell<sup>(3)</sup>

(1) previously with UCSB, now with The Johns Hopkins University Applied Physics Laboratory, 11100 Johns Hopkins Road, Laurel, Maryland 20723

(2) previously with UCSB, now with Teledyne Scientific & Imaging, LLC  
1049 Camino Dos Rios, Thousand Oaks, CA 91360

(3) Department of Electrical and Computer Engineering,  
University of California, Santa Barbara, CA 93106

E-mail: colin.sheldon@jhuapl.edu

### Abstract

A scalable system architecture is proposed and demonstrated for spatial multiplexing over millimeter-wave line-of-sight communication links. The architecture decouples spatial channel separation from demodulation, allowing the system bandwidth and data rates to scale up, while performing spatial processing on a time scale matched to the slow time variations of the spatiotemporal channel. The spatially multiplexed channels are separated at the receiver using broadband adaptive analog  $I/Q$  vector signal processing. A control loop continuously tunes the channel separation electronics to correct for changes with time in either the propagation environment or the system components. Design and characterization of a four-channel 60 GHz hardware prototype operating at 2.4 Gb/s is presented. This result is the highest data rate line-of-sight wireless link employing adaptive spatial multiplexing reported to date.

### Introduction

Spatial multiplexing provides a mechanism for increasing the data rate of a radio link without increased channel bandwidth. Research in this area has focused primarily on WiFi (e.g., 802.11n) and cellular (e.g., WiMAX and LTE) systems operating at low GHz carrier frequencies, where spatial multiplexing requires a rich scattering environment. In contrast, the 60 GHz system reported here demonstrates that, for small carrier wavelengths, spatial multiplexing can be achieved even in line-of-sight (LOS) environments with moderate antenna separations. Fixing the size of the antenna array, the maximum number of spatially multiplexed channels varies as the inverse of carrier wavelength  $\lambda$  for a linear array and as  $1/\lambda^2$  for rectangular arrays. Operation at millimeter wave frequencies simultaneously provides a short carrier wavelength and the ability to take advantage of the large swathes of unlicensed and semi-unlicensed bandwidth at 60 GHz and 71-95 GHz. We anticipate that data rates far exceeding 10 Gb/s are feasible using a combination of spatial multiplexing and large channel bandwidths, in contrast to data rates well below 1 Gb/s at lower carrier frequencies [1].

We present a scalable architecture that allows channel bandwidth and data rates to increase while allowing processing for spatial channel separation to occur on a slow time scale matched to the slow variations in the spatial channel. We have previously reported experimental results for a system using a two element array at each end with manually tuned channel separation at IF [2]. In this paper, we report a system with a four element linear array at each end, with automatically tuned baseband channel separation. New

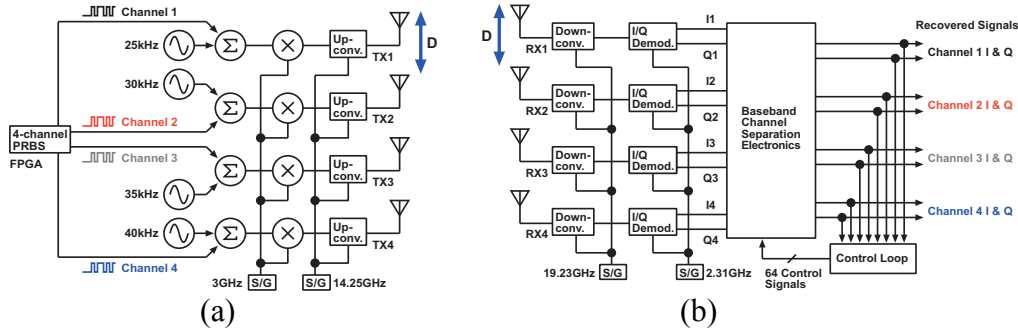


Fig. 1: Transmitter (a) and receiver (b) hardware prototype.

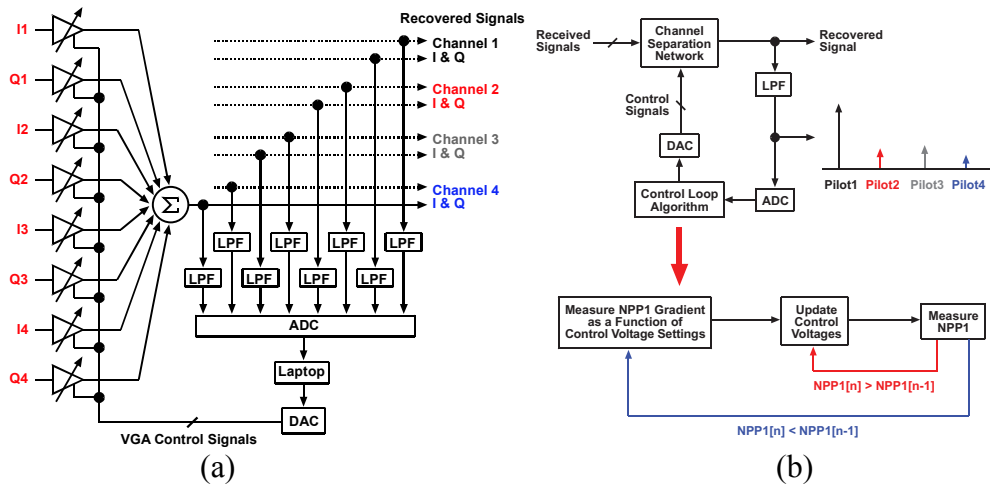


Fig. 2: Baseband CSN hardware (a) and control loop (b).

results are reported here for an enhanced prototype operating at 2.4 Gb/s with similar BER performance to initial work at 400 Mb/s [3].

### Four Channel Hardware Prototype

The hardware prototype (Fig. 1) consisted of a four channel (1×4) transmitter and a four element receiver and used commercially available mm-wave and RF components. Unique pilot tones were added to each PRBS sequence prior to transmission. The receiver used an analog baseband channel separation network and a low-speed digital control loop to recover the transmitter channels prior to data demodulation (Fig. 2).

The baseband channel separation network (CSN) consisted of custom printed circuit boards (Fig. 2a). Each PCB contained 8 variable gain amplifiers (VGAs) implemented as full four quadrant analog multipliers, allowing arbitrary magnitude scaling and phase shift operations on each of the received signals.

The baseband channel separation control loop (Fig. 2b) adjusts the baseband VGA coefficients to retain the channel of interest and suppress the interfering channels. The eight outputs of the CSN are filtered and digitized at 125 Ksamples/s to measure the magnitude of the embedded transmitter pilot tones. The sampling rate is determined by the pilot tones frequencies (25, 30, 35, 40 KHz) and not by the data rate (600 Mb/s per

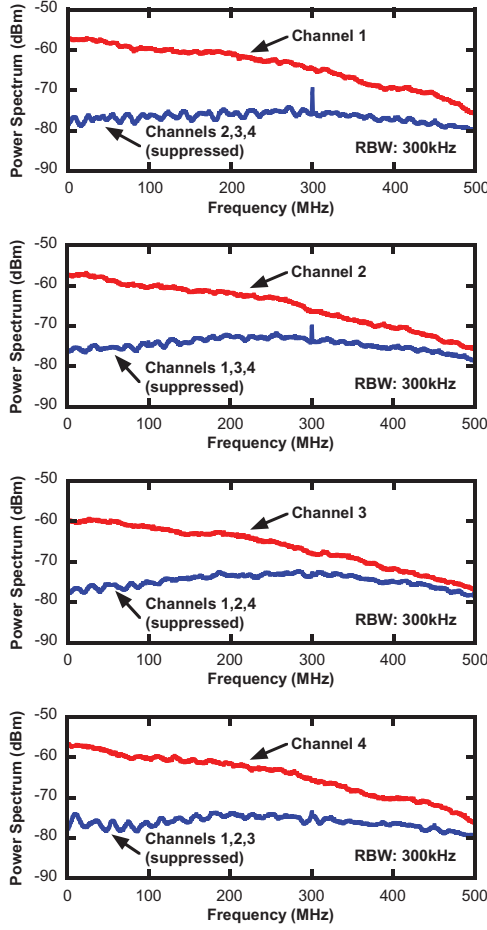


Fig. 3: Measured CSN performance.

channel). These frequencies are above the  $\sim 1$  KHz low frequency cut off of the receiver chain and are low enough to allow the use of a low cost multi-channel digitizer.

The magnitude of the pilot tones at the outputs of the CSN are measured and the interference channel power at CSN output  $k$  is given by

$$NPP_k = \frac{P_{k,k}}{P_{k,1} + P_{k,2} + P_{k,3} + P_{k,4}} \quad (1)$$

where  $NPP_k$  is the normalized pilot power at CSN output  $k$  and  $P_{k,j}$  is the pilot power from transmitter  $j$  present in CSN output  $k$ . It follows that for ideal channel separation,  $NPP_k = 1$ , when  $P_{k,j} = 0$  for all  $k \neq j$ . The control loop attempts to find the optimum VGA coefficients for CSN  $k$  using a simple gradient based iteration (Fig. 2b).

Several enhancements were made to the initial four channel prototype [3]. Transmitter power was increased. The transmitter and receiver electronics were modified to remove standing waves in the hardware that caused gain ripples in the system transfer function, limiting the system data rate. These improvements to the prototype increased the system data rate from 100 Mb/s per channel to 600 Mb/s per channel.

The baseband CSN and control loop (Fig. 2) were expanded to allow simultaneous recovery of  $I/Q$  signals for all four transmitter channels. Pilot tone frequencies were

TABLE I  
LINK BUDGET

TX Antenna Gain	24	dB <sub>i</sub>
RX Antenna Gain	24	dB <sub>i</sub>
Link Range	5	m
Free-Space Path Loss	82	dB
RX Noise Figure	14	dB
Bit Error Rate	$10^{-6}$	
Link Margin	17	dB
TX Power	-10	dBm
RX Power	-44	dBm

TABLE II  
SUMMARY OF EXPERIMENTAL RESULTS

Recovered Channel	BER	Signal-to-Interference Ratio (dB)
1	$< 10^{-6}$	15
2	$< 10^{-6}$	12
3	$1.2 \times 10^{-5}$	10
4	$< 10^{-6}$	14

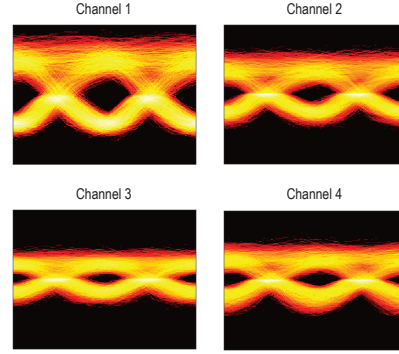


Fig. 4: Measured eye patterns.

reduced to 25-40 kHz to allow the use of a low cost multi-channel digitizer in the channel separation control loop. The shared transmitter and receiver local oscillator reference signal used in previous experiments with the initial prototype [3] was removed. Carrier recovery was not implemented at the receiver. The control loop algorithm was modified to operate in the presence of unlocked and drifting transmitter and receiver local oscillator frequencies. Offline Differential PSK (DPSK) demodulation was performed on stored copies of the recovered  $I/Q$  signals for each channel.

### Experimental Results

The hardware prototype was tested in an indoor office environment at a 5 m link range. The antenna element spacing was 7.9 cm at both the transmitter and receiver. Table 1 is a summary of the link budget. System performance was characterized in the frequency domain and with BER testing. The  $I$  and  $Q$  components of one recovered channel were simultaneously captured using a two channel oscilloscope. DPSK data demodulation and BER testing were performed offline on the captured signals.

CSN performance was measured in the frequency domain by transmitting 600 Mb/s PRBS sequences. The received power spectrum was measured at the output of the CSN under two conditions: transmitting a single channel and transmitting the three interfering channels with the channel of interest turned off. Fig. 3 is a plot of the measured power spectrums for each channel under both conditions. Table 2 summarizes the measured signal to interference ratio (SIR) for each channel. BER testing was performed using 600 Mb/s PRBS signals. The BER was measured under two conditions: transmitting one channel at a time and transmitting all four channels simultaneously. For the case of a single active transmitter, the BER was  $< 10^{-6}$  for all channels. The measured BER when all four channels were transmitting is summarized in Table 2. Fig. 4 shows typical eye patterns after DPSK demodulation. System performance was similar to initial experiments [3], despite the increase in data rate from 100 Mb/s to 600 Mb/s per channel and the unlocked transmitter and receiver local oscillators. SIR and BER performance were similar for channels 1,2, and 4. Channel 3 suffered reduced SIR performance and an increased BER compared to the other channels. Further work is needed to determine the source of the poor channel 3 performance.

### Conclusion

This work demonstrates an architecture for LOS mm-wave communication systems that scales well with bandwidth and the number of parallel spatial channels. Pilot tones were used with adaptive signal processing to implement channel separation using low-speed baseband electronics. Key to the scalability is the decoupling of channel separation (which can be adapted slowly) from the high-rate processing required for each multi-gigabit data channel after separation.

### References

- [1] M. Zargari, et al., "A Dual-Band CMOS MIMO Radio SoC for IEEE 802.11n Wireless LAN," *IEEE J. Solid-State Circuits*, vol.43, no.12, pp.2882-95, Dec. 2008.
- [2] C. Sheldon, et al., "A 60GHz Line-of-Sight 2x2 MIMO Link Operating at 1.2Gbps," *IEEE Int. AP-S Sym.*, July 2008.
- [3] C. Sheldon, et al., "Four-Channel Spatial Multiplexing Over a Millimeter-Wave Line-of-Sight Link," *IEEE MTT-S Int. Microwave Sym.*, June 2009.